Rta of murine gammaherpesvirus 68 reactivates the complete lytic cycle from latency

JOURNAL OF VIROLOGY, Apr. 2000, p. 3659–3667 Vol. 74, No. 8
0022-538X/00/$04.00+0

Rta of Murine Gammaherpesvirus 68 Reactivates the Complete Lytic Cycle from Latency

TING-TING WU,[1] EDWARD J. USHERWOOD,[2] JAMES P. STEWART,[3] ANTHONY A. NASH,[3] AND REN SUN[1]*

Department of Molecular and Medical Pharmacology, the UCLA AIDS Institute, the Jonsson Comprehensive Cancer Center, and the Molecular Biology Institute, University of California at Los Angeles, Los Angeles, California 90095[1]; The Trudeau Institute, Saranac Lake, New York 12983[2]; and Department of Veterinary Pathology, University of Edinburgh, Edinburgh EH9 1QH, United Kingdom[3]

Received 7 October 1999/Accepted 21 January 2000

Herpesviruses are characterized as having two distinct life cycle phases: lytic replication and latency. The mechanisms of latency establishment and maintenance, as well as the switch from latency to lytic replication, are poorly understood. Human gammaherpesviruses, including Epstein-Barr virus (EBV) and human herpesvirus-8 (HHV-8), also known as Kaposi's sarcoma-associated herpesvirus (KSHV), are associated with lymphoproliferative diseases and several human tumors. Unfortunately, the lack of cell lines to support efficient de novo productive infection and restricted host ranges of EBV and HHV-8 make it difficult to explore certain important biological questions. Murine gammaherpesvirus 68 (MHV-68, or γHV68) can establish de novo lytic infection in a variety of cell lines and is also able to infect laboratory mice, offering an ideal model with which to study various aspects of gammaherpesvirus infection. Here we describe in vitro studies of the mechanisms of the switch from latency to lytic replication of MHV-68. An MHV-68 gene, *rta* (replication and transcription activator), encoded primarily by open reading frame 50 (ORF50), is homologous to the *rta* genes of other gammaherpesviruses, including HHV-8 and EBV. HHV-8 and EBV Rta have been shown to play central roles in viral reactivation from latency. We first studied the kinetics of MHV-68 *rta* gene transcription during de novo lytic infection. MHV-68 *rta* was predominantly expressed as a 2-kb immediate-early transcript. Sequence analysis of MHV-68 *rta* cDNA revealed that an 866-nucleotide intron 5′ of ORF50 was removed to create the Rta ORF of 583 amino acids. To test the functions of MHV-68 Rta in reactivation, a plasmid expressing Rta was transfected into a latently infected cell line, S11E, which was established from a B-cell lymphoma in an MHV-68-infected mouse. Rta induced expression of viral early and late genes, lytic replication of viral DNA, and production of infectious viral particles. We conclude that Rta alone is able to disrupt latency, activate viral lytic replication, and drive the lytic cycle to completion. This study indicates that MHV-68 provides a valuable model for investigating regulation of the balance between latency and lytic replication in vitro and in vivo.

Latency provides unique advantages for herpesviruses to escape host immune surveillance and to establish lifelong persistent infections. However, to maintain viral reservoirs and transmit to other hosts, herpesviruses must be reactivated from latency and enter the lytic replication phase to generate more virus. The balance between viral latency and lytic replication is therefore a critical factor that determines the outcome of infection and the corresponding pathogenesis. If the balance favors lytic replication, lytic infections of herpes simplex virus sometimes lead to morbidity through encephalitis or visual loss through keratoconjunctivitis (43). On the other hand, if the balance favors viral latency, latent infection by Epstein-Barr virus (EBV) can cause lymphoproliferative diseases (29).

The physiological signals that cause reactivation of herpesviruses are not well understood. The molecular mechanisms of reactivation have been most extensively investigated in two human gammaherpesviruses, EBV and human herpesvirus 8 (HHV-8). Most of these studies have been carried out in B-cell lymphoma-derived cell lines harboring the latent virus. In EBV, two viral gene products, ZEBRA and Rta, are expressed earliest upon reactivation induced by chemical or biological agents (21, 25, 33, 37) and activate viral promoters triggering lytic gene expression (1–3, 5, 6, 11, 12, 14). To study the functions of ZEBRA and Rta in reactivation, plasmids expressing ZEBRA and Rta were transfected into latently infected B-cell lines to determine whether expression of viral lytic genes and lytic replication of viral DNA were activated. ZEBRA alone is able to activate viral lytic cycle in B cells and epithelial cells latently infected with EBV (5, 15, 19). Rta synergizes with ZEBRA to promote activation of viral lytic gene expression (3, 6, 27, 44), but does not always disrupt latency by itself. In certain latently infected B-cell and epithelial cell lines, Rta can disrupt viral latency (28, 44). ZEBRA and Rta act as transcriptional activators in transient transfection assays with reporter constructs. Moreover, ZEBRA and Rta have been shown to stimulate expression, not only of themselves, but of each other (8, 28, 32, 44, 45), although the levels of activation vary, depending upon the experimental system used. Therefore, it has been proposed that ZEBRA and Rta function in a cooperative manner to activate the viral lytic cycle.

The HHV-8 homologue of EBV Rta has been shown to be sufficient to activate expression of early and late viral lytic genes in B-cell lines latently infected with HHV-8; however, it has not been demonstrated whether viral lytic DNA replication or virus production can be induced (17, 35). Upon reactivation, HHV-8 *rta* is expressed as an immediate-early gene, but the

* Corresponding author. Mailing address: Department of Molecular and Medical Pharmacology, University of California at Los Angeles, Los Angeles, CA 90095-1735. Phone: (310) 794-5557. Fax: (310) 794-5123. E-mail: rsun@mednet.ucla.edu.

zebra homologue of HHV-8 is an early gene. Moreover, HHV-8 ZEBRA is not able to disrupt latency (35). Although the roles of ZEBRA and Rta in reactivation of EBV or HHV-8 have been investigated, their expression and functions during de novo lytic infection cannot be studied, because there is no efficient in vitro system available. In addition, the lack of an effective animal model has made studies of gammaherpesvirus reactivation in vivo almost impossible.

Murine gammaherpesvirus 68 (MHV-68, also referred to as γHV68), which is phylogenetically related to HHV-8 and EBV, offers an excellent model in which to study the mechanisms underlying the dynamic balance between latency and lytic replication (40). In vitro cell culture systems are available to study de novo lytic infection, latency, and reactivation of MHV-68. Moreover, MHV-68 can establish lytic and latent infection in laboratory mice (36), which allows us to address questions regarding the host-virus interactions (22, 23, 30, 33). MHV-68 forms plaques on monolayers of many cell lines, making it relatively easy to genetically manipulate the viral genome. This also makes it possible to examine the functions of individual viral genes in various aspects of the viral life cycle, including reactivation.

The molecular mechanisms of MHV-68 reactivation, however, have not been previously characterized. Efforts have been made to identify the *zebra* homologue in MHV-68, but so far have not been successful. On the other hand, the *rta* homologue is readily found in MHV-68 (18), and, in fact, *rta* is conserved among gammaherpesviruses, including EBV, HHV-8, herpesvirus saimiri (HVS), and bovine herpesvirus 4 (BHV-4). This led us to test the hypothesis that MHV-68 Rta may be the central viral factor governing reactivation. In this study, the kinetics of MHV-68 *rta* transcription during de novo lytic infection were first examined. Next, the functions of MHV-68 Rta in reactivation were studied by using a B-cell line harboring latent MHV-68. Our results indicate that MHV-68 *rta* is expressed as an immediate-early gene during de novo lytic infection and is capable of initiating viral lytic replication in latently infected B cells.

MATERIALS AND METHODS

Viruses, cells, and plaque assays. MHV-68 was originally obtained from the American Type Culture Collection (VR1465), and the working stocks were grown by infecting BHK-21 cells (ATCC CCL-10) at 0.1 PFU per cell. BHK-21 cells were maintained in Dulbecco's modified Eagle's medium (DMEM) containing 10% fetal bovine serum (FBS). S11E is a clonal cell line of S11, which was established from a B-cell lymphoma developed in an MHV-68-infected mouse and contains latent MHV-68 (38). S11E was cloned on the basis of a low spontaneous reactivation frequency (13). S11E cells were cultured in RPMI 1640 medium containing 15% FBS. To infect BHK-21 cells, the viral inoculum in DMEM was incubated with cells for 1 h with occasional swirling. The inoculum was removed and replaced with fresh DMEM plus 10% FBS. For the experiments involving cycloheximide (Sigma, St. Louis, Mo.) (see Fig. 2), cells were treated at a concentration of 100 or 200 μg/ml 1 h prior to, during, and after viral inoculation until they were harvested. For the experiments using phosphonoacetic acid (PAA) (Sigma) (Fig. 2), cells were treated at a concentration of 200 μg/ml after viral inoculation until they were harvested.

The viral titers were measured by plaque assays, using monolayers of BHK-21 cells overlaid with 1% methylcellulose (Sigma) for 5 days. The cells were fixed and stained with 2% crystal violet in 20% ethanol. Plaques were then counted to determine the titers. To measure the viral titers in the supernatants of transfected S11E cells, the suspension cultures of cells were centrifuged twice at 450 × *g*, and the supernatants were harvested for plaque assays.

RT-PCR, DNA cloning, and sequencing. For reverse transcription (RT), 0.5 μg of 22-mer oligo(dT) and 2 μg of total RNA isolated from BHK-21 cells infected with MHV-68 (2 PFU/cell) at 8 h postinfection were first denatured at 70°C for 10 min, immediately placed on ice, and incubated with 200 U of Superscript II (Gibco BRL, Gaithersburg, Md.) at 42°C for 1 h. Ten percent of the product was then amplified by PCR, with primers R3 (5′-CTGAATTCGCAGCG**ATG**GCC TCTGACTC-3′, containing an *Eco*RI site [underlined] and the Kozak's sequence upstream of the translation initiation codon [boldface], corresponding to nucleotide [nt] 66760) and R4 (5′-GATCTAGACCGT**TTA**TGACTCCAGGCT G-3′, containing an *Xba*I site [underlined] upstream of the termination codon [boldface], corresponding to nt 69374). The RT-PCR product was reamplified by using R3 and another primer internal to R4, R6 (5′-GATATGTACCCACATG GATGCCTGT-3′, corresponding to nt 67974 to 67950). The resulting product was cloned into the pCR2.1 T-vector (Invitrogen, Carlsbad, Calif.). The positive colonies were selected by blue-white screening, and plasmid DNA from those colonies was isolated for DNA sequencing with primer R7 (5′-CATCTTCAGG GTGCTGTAGGAA-3′, corresponding to nt 67781 to 67760). The nucleotide numbering is according to Virgin et al. (40), and the relative positions of the primers to open reading frame 50 (ORF50) are indicated in Fig. 1C. To construct an Rta expression vector, the *rta* genomic sequence was amplified by PCR with primers R3 and R4 from total DNA isolated from MHV-68-infected BHK-21 cells. The 2.6-kb PCR product was subjected to *Xba*I digestion followed by *Eco*RI digestion and then cloned into a pcDNA3 vector (Invitrogen) containing the cytomegalovirus immediate-early promoter and enhancer.

RNA extraction and Northern analysis. Total RNA was extracted from BHK-21 or S11E cells by the guanidinium-acid phenol method, as described by Chomczynski and Sacchi (4). RNA was treated with a mixture of 1 M glyoxal and 50% (vol/vol) dimethyl sulfoxide at 50°C for 30 min (7). Glyoxalated RNA was then separated on 1% agarose gels in circulating 10 mM sodium phosphate buffer (pH 6.8). A 1-kb ladder (Gibco BRL) and λ *Hin*dIII were 5′ end labeled with [γ-^{32}P]dATP, glyoxalated, and loaded onto the gels as the size standards. RNAs on gels were transferred to charged nylon membranes (Amersham Pharmacia Biotech, Arlington Heights, Ill.). The membranes were UV cross-linked and deglyoxalated at 80°C in 20 mM Tris-HCl (pH 8). Prehybridization and hybridization were carried out at 65°C in 0.5 M K_2HPO_4 (pH 6.8) containing 7% sodium dodecyl sulfate (SDS) and 1% bovine serum albumin. The probes were generated by the random-priming method with [α-^{32}P]dCTP with the templates generated by PCR of viral genomic DNA. The membranes were then washed at 65°C with 40 mM sodium phosphate (pH 6.8) containing 5% SDS and 0.5% bovine serum albumin, followed by washing with 40 mM sodium phosphate (pH 6.8) containing 0.5% SDS. Radioactivity was detected and quantitated with a STORM imaging system (Molecular Dynamics, Sunnyvale, Calif.). Before rehybridization with a different probe, the membranes were stripped at 80°C in 10 mM Tris-HCl (pH 8) containing 1% SDS.

Transfection. Transfection of S11E cells was carried out by electroporation. S11E cells (10^7) and 10 μg of plasmid DNA were mixed in a cuvette (Bio-Rad, Hercules, Calif.) and shocked in a Gene-Pulser II (Bio-Rad). To monitor transfection efficiencies, 2 μg of plasmid pEGFP-C1 (Clontech, Palo Alto, Calif.) was included in each transfection, and the percentage of cells expressing green fluorescent protein was determined at 24 h posttransfection by fluorescent microscopy.

Western analysis. Cells were lysed in Laemmli buffer containing 0.25 M Tris-HCl (pH 6.8), 2% SDS, 10% glycerol, 5% β-mercaptoethanol, and 0.002% bromophenol blue. The lysates were heated to 95°C and subjected to electrophoresis on 10% polyacrylamide gels. The broad-range prestained protein standard (Bio-Rad) was also loaded onto the gels. Proteins on gels were electrotransferred (Bio-Rad) onto nitrocellulose membranes (Amersham Pharmacia Biotech). The membranes were blocked in phosphate-buffered saline (PBS) plus 0.1% Tween 20 and 5% milk, incubated with the rabbit hyperimmune serum against MHV-68-infected rabbit cells (36), washed in PBS containing 0.1% Tween 20, and incubated with antirabbit immunoglobulin G conjugated with horseradish peroxidase. The proteins were detected with the enhanced chemiluminescence detection ECL+PLUS system (Amersham Pharmacia Biotech), and the signals were imaged with a STORM imaging system (Molecular Dynamics).

DNA extraction and Southern analysis. Total DNA was harvested by lysing cells in the buffer containing 10 mM Tris-HCl (pH 8), 50 mM EDTA (pH 8), and 0.5% SDS. The lysates were incubated with proteinase K (100 μg/ml) at 50°C overnight and then extracted twice with phenol-chloroform (1:1). DNA was precipitated with ammonium acetate and ethanol, and the DNA pellet was dissolved in Tris-EDTA buffer (pH 8). Total DNA was subjected to restriction enzyme digestion overnight and electrophoresed on 0.8% agarose gels. Gels were stained with ethidium bromide to visualize DNA and then subjected to depurination, denaturation, and neutralization. DNAs on treated gels were transferred to charged nylon membranes (Amersham Pharmacia Biotech). The membranes were UV cross-linked and prehybridized at 68°C in the buffer containing 5× SSC (1× SSC is 0.15 M NaCl plus 0.015 M sodium citrate), 10× Denhardt's solution, 0.5% SDS, and denatured salmon sperm DNA (50 μg/ml). Probes were generated by the random priming method using [α-^{32}P]dCTP and PCR products of genomic viral DNA as templates. The membranes were washed at 68°C in 2× SSC with 0.1% SDS, followed by 0.1× SSC with 0.1% SDS. Radioactivity was detected and quantitated by using a STORM imaging system (Molecular Dynamics).

RESULTS

The structure of the *rta* gene. MHV-68 ORF50 was previously shown to share homology to ORF50 of HHV-8, EBV,

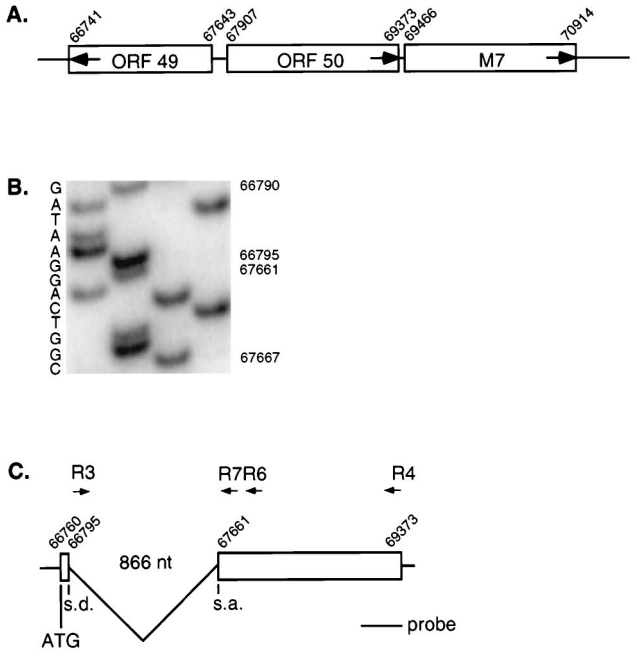

FIG. 1. Structure of the MHV-68 *rta* gene. (A) Genomic location of ORF50. The nucleotide numbers are assigned on the basis of the MHV-68 sequence in the National Center for Biotechnology Information database (40). The open boxes represent ORFs predicted by computer analysis, and the numbers assigned to individual ORFs are based on homology with the corresponding ORFs of HVS and HHV-8 (40). The arrows in the open boxes indicate the orientation of ORFs. A major portion of the *rta* gene is carried by ORF50. Downstream of ORF50 is ORFM7 encoding gp150, which shares homology with EBV gp350 (34). (B) Sequencing analysis of the *rta* cDNA. RNA harvested from BHK-21 cells infected with MHV-68 at 2 PFU/cell was reverse transcribed with oligo(dT) and amplified, first by primers R3 and R4 and then by primers R3 and R6. The resultant product was cloned, and the positive clone was sequenced with the R7 primer. The splice donor and acceptor sites were mapped to nt 66795 and 67661, respectively. (C) Splicing of the *rta* gene. The splice donor (s.d.) and splice acceptor (s.a.) sites were localized to nt 66795 and 67661, respectively. An intron of 866 nt is removed, and two exons are joined together to generate the Rta ORF, with the translation initiation codon at nt 66760. Primers R3 and R4 were used for PCR amplification of the cDNA product and the genomic sequence spanning the *rta* gene. R3 and R6 were used to reamplify the cDNA PCR product of R3 and R4 for cloning. R7 was used to sequence the splicing junction. The probe shown in panel C was used for Northern analysis of the *rta* transcripts shown in Fig. 2A.

and HVS (18, 40). The genomic location of ORF50 is shown in Fig. 1A. ORF50 encodes the major portion of the *rta* homologue of gammaherpesviruses. The *rta* genes of HHV-8, EBV, HVS, and BHV-4 share one common feature: the second exon containing ORF50 is spliced to the first exon by removing an intron carrying ORF49 (17, 19, 35, 39, 41). Because of the conservation of the splicing event, we hypothesized that the *rta* gene of MHV-68 undergoes similar RNA processing. To confirm this, total RNA was isolated from MHV-68-infected BHK-21 cells and reverse transcribed with oligo(dT), followed by PCR, with primers flanking ORF50 (R3 and R4). The resultant RT-PCR product was ~1.7 kb and smaller than the PCR product (2.6 kb) generated with the same pair of primers, but with genomic DNA as the template, consistent with RNA splicing (data not shown). To precisely determine the splicing junction, the RT-PCR product was reamplified with primer R3 and another primer, R6 (internal to R4), and then cloned and sequenced with the R7 primer. As shown in Fig. 1B, the splicing donor and acceptor sites are located at nt 66795 and 67661, respectively (numbering according to the National Center for Biotechnology Information database [40]). The sequences flanking nt 66795 and 67661 were highly homologous to the consensus sequences flanking the splice donor and acceptor sites, respectively. As a result of splicing, an 866-nt intron containing the entire ORF49 was removed (Fig. 1C). Instead of the predicted methionine of ORF50 (40), the translation initiation methionine of MHV-68 *rta* would be located in the 5′ small exon at nt 66760. Consequently, MHV-68 Rta would have an extra 94 amino acids (aa) added to the N terminus of ORF50 (489 aa).

MHV-68 *rta* was expressed as an immediate-early transcript. To examine the kinetics of MHV-68 *rta* transcription during de novo infection, BHK-21 cells were infected at 5 PFU/cell, and total RNA was harvested at different times postinfection. In addition, infections were carried out in the presence of 100 or 200 μg of cycloheximide per ml (a protein synthesis inhibitor) or 200 μg of PAA per ml (a herpesvirus DNA polymerase inhibitor). The *rta* transcripts were analyzed by Northern blotting with the 0.7-kb PCR fragment spanning the C terminus of ORF50 (corresponding to nt 68651 to 69378; Fig. 1C) as a probe. As shown in Fig. 2A, a major band of 2.0 kb was detected at the earliest time point, 2 h postinfection (Fig. 2A, lane 4). Expression of the 2-kb transcript peaked at 4 h postinfection (Fig. 2A, lane 5) and decreased at 8 h postinfection (Fig. 2A, lane 6). In the presence of cycloheximide, the 2-kb transcript was still detected (Fig. 2A, lanes 7 and 8), consistent with the expression pattern of an immediate-early gene.

A single-stranded RNA probe was used for Northern analysis (data not shown) and confirmed that the orientation of the 2-kb transcript was the same as that of ORF50. This 2.0-kb transcript would be large enough to encode the entire ORF of Rta (583 aa). The 0.7-kb probe also detected a few minor larger transcripts, one of which was deduced to be 3.4 kb and only appeared in the cells treated with cycloheximide (Fig. 2A, lanes 7 and 8). Other transcripts appeared later than the major 2-kb transcript, and their expression was abolished in the presence of cycloheximide (Fig. 2A, lanes 7 and 8), as well as in the presence of PAA (Fig. 2A, lane 11), indicating that they were late viral transcripts.

The same membrane was stripped and rehybridized with a probe derived from the thymidine kinase (TK) ORF (Fig. 2B). Several transcripts were detected, with three predominant species of 2.1, 2.6, and 3.8 kb. The major 2.6-kb species was detected at 2 h postinfection (Fig. 2B, lane 2) and was expressed earlier than the other species of 2.1, 2.8, 3.2, and 3.8 kb, but disappeared at 8 h postinfection (Fig. 2B, lane 6). Its expression, however, was sensitive to cycloheximide treatment (Fig. 2B, lanes 7 and 8), indicating that this was an early viral transcript. The minor 3.2-kb species was expressed at kinetics similar to those of the major 2.6-kb transcript and was also an early viral transcript. Other species of transcripts, including the other major 2.1- and 3.8-kb transcripts, continued to accumulate until 13 h postinfection and then decreased at 24 h postinfection. However, their expression was inhibited by the presence of PAA (Fig. 2B, lane 11), leading to the conclusion that the other species were late viral transcripts. Our results are consistent with a previous study in which several TK-related transcripts were detected, including a 2.6-kb transcript, and the expression pattern of this 2.6-kb transcript was characteristic of an early gene (26).

The membrane was rehybridized with a probe derived from the M9 ORF (Fig. 2C). MHV-68 M9 has homology to ORF65 of HHV-8 (40), which encodes a capsid protein. Several species of RNAs were detected, including two major transcripts of 0.9 and 3.6 kb, which were observed at 4 h postinfection,

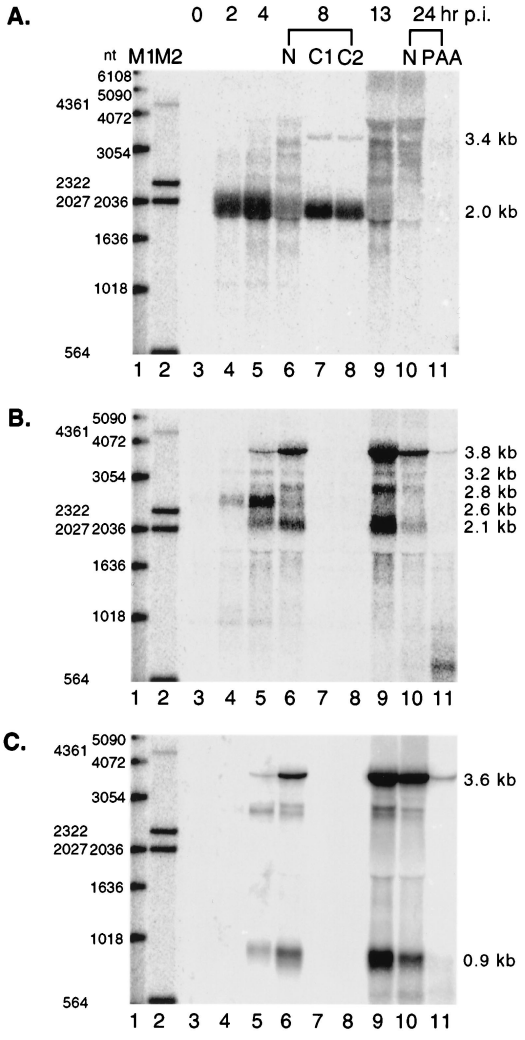

FIG. 2. MHV-68 *rta* is expressed as an immediate-early gene. Infection was carried out in six-well plates, and RNA was harvested at various times postinfection (p.i.), as indicated at the top of the panels. Half of the total cellular RNA was glyoxalated and subjected to Northern analysis. In each panel, lanes 1 and 2 are a 1-kb DNA ladder and λ *Hin*dIII, respectively; the sizes of the individual bands are indicated to the left. RNA was collected at 0 (lane 3), 2 (lane 4), 4 (lane 5), or 13 (lane 9) h postinfection. RNA was harvested from cells at 8 h postinfection without (lane 6 [N]) or with cycloheximide treatment at 100 (lane 7 [C1]) or 200 (lane 8 [C2]) μg/ml. At 24 h postinfection, RNA was isolated from cells without (lane 10 [N]) or with (lane 11) 200 μg of PAA per ml added to the medium. The same membrane was hybridized with three different probes, as shown in the three panels. The probe used in panel A was derived from the very last 0.7-kb sequence (nt 68651 to 69378) or ORF50, which was generated by *Sac*I digestion of the PCR product amplified with the R3 and R4 primers. Panel B shows the image of the membrane rehybridized with the probe derived from the PCR product spanning the 1.9-kb TK ORF (nt 32879 to 34813). The probe used in panel C was derived from the PCR product of the 0.5-kb M9 ORF (nt 93962 to 94522). The deduced sizes of the transcripts are indicated to the right of each panel. Radioactivity was detected with a STORM imaging system.

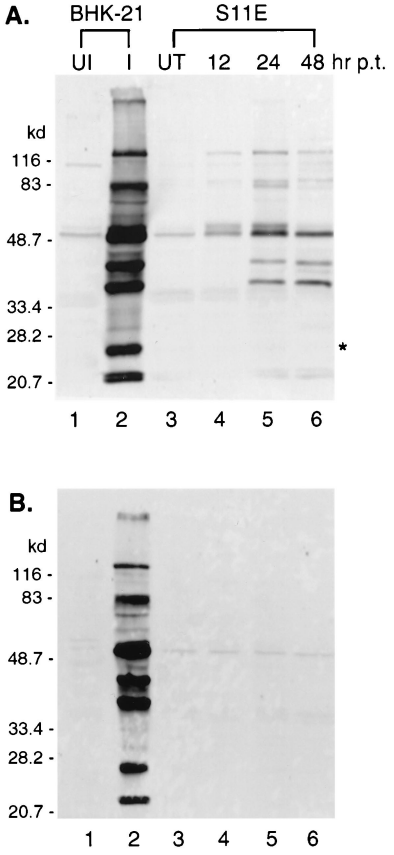

FIG. 3. Induction of viral lytic proteins by Rta. S11E cells (10^7) were electroporated with pcDNA3/MHV-68 *rta* (A) or pcDNA3 (B). Total protein from 10^5 cells was collected at 12 (lanes 4 of panels A and B), 24 (lanes 5 of panels A and B), or 48 (lanes 6 of panels A and B) h posttransfection (p.t.). Proteins from 10^4 uninfected (UI [lane 1]) or MHV-68-infected (I [lane 2]) BHK-21 cells or from 10^5 untransfected S11E cells (UT [lanes 3]) were loaded and subjected to Western analysis with the rabbit hyperimmune serum against MHV-68-infected rabbit cell lysates. The molecular masses (kilodaltons) of individual proteins in the marker are indicated to the left.

gradually increased until 13 h postinfection and then declined by 24 h postinfection. Their expression was abrogated by treatment with PAA (Fig. 2C, lane 11), indicating that they were late viral transcripts. Two minor transcripts of 2.8 and 2.9 kb were also observed. The 2.8-kb RNA was detected at 4 h and disappeared at 24 h postinfection, and the 2.9-kb RNA was not visible until 8 h, and continued to accumulate until 13 h postinfection. Expression of both RNAs was sensitive to the presence of PAA (Fig. 2C, lane 11), indicating that, like the two major transcripts, these two minor transcripts were late viral RNAs.

MHV-68 Rta activated viral lytic gene expression in latently infected S11E cells. To study the function of MHV-68 Rta, the 2.6-kb sequence (nt 66760 to 69373) spanning the initiation methionine and the termination codon was cloned into a eukaryotic gene expression vector, pcDNA3, where expression was driven by the cytomegalovirus immediate-early promoter. Since *rta* was expressed as an immediate-early gene during de novo lytic infection, we tested whether Rta could disrupt latency and initiate the cascade of lytic gene expression. pcDNA3/MHV-68 *rta* was transfected into an MHV-68 latently infected B-cell line, S11E, and transfection efficiency was determined by the percentage of cells expressing green fluorescent protein encoded by a cotransfected plasmid, ranging from 5 to 10%.

Transfected S11E cells were harvested at different times posttransfection for Western analyses by using the rabbit hyperimmune serum raised against MHV-68-infected rabbit cell lysates, and the results are shown in Fig. 3. Transfection of pcDNA3/MHV-68 *rta* (Fig. 3A) into S11E cells induced the expression of a variety of proteins, which were also seen in

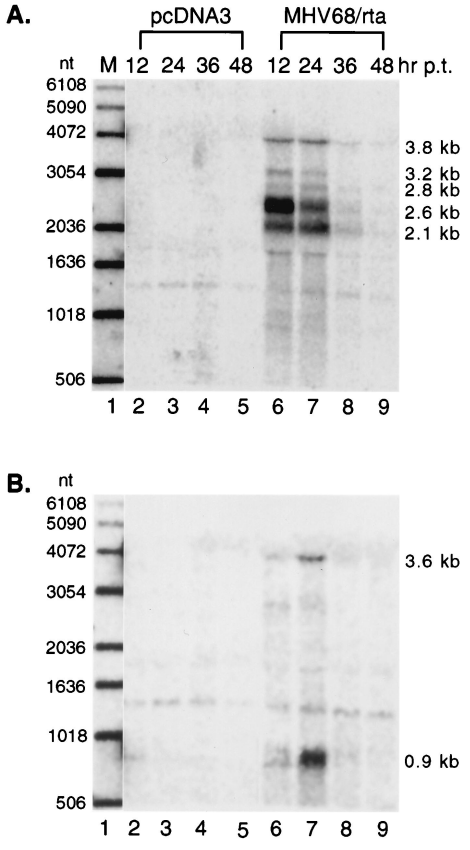

FIG. 4. Activation of viral lytic gene expression by Rta. RNA from S11E cells electroporated with pcDNA3 (lanes 2 to 5) or pcDNA3/MHV-68 *rta* (lanes 6 to 9) was collected at 12 (lanes 2 and 6), 24 (lanes 3 and 7), 36 (lanes 4 and 8), or 48 (lanes 5 and 9) h posttransfection (p.t.). Half of the total cellular RNA was glyoxalated and subjected to Northern analysis. The same membrane hybridized with different probes is shown in two panels. The probe used in panel A is derived from the TK ORF (as in Fig. 1B). In panel B, the probe is derived from the M9 ORF (as in Fig. 1C). Lane 1 is a 1-kb DNA ladder, with the sizes of individual bands indicated to the left. The deduced sizes of transcripts are indicated to the right. Radioactivity was detected with a STORM imaging system.

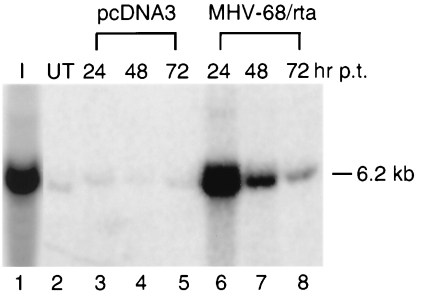

FIG. 5. Amplification of viral DNA by Rta. Total DNA from 2×10^6 S11E cells transfected with pcDNA3 (lanes 3 to 5) or pcDNA3/MHV-68 *rta* (lanes 6 to 8) was harvested at 24 (lanes 3 and 6), 48 (lanes 4 and 7), or 72 (lanes 5 and 8) h posttransfection (p.t.) and subjected to digestion with *Hin*dIII. The digested DNAs were electrophoresed on a 0.7% agarose gel for Southern analysis. *Hin*dIII-digested DNA from 5×10^5 MHV-68-infected BHK-21 cells was loaded in lane 1 as a positive control (I), and digested DNA from 2×10^6 untransfected S11E cells was loaded in lane 2 as a negative control (UT). The probe used to detect the viral DNA was derived from the 6.2-kb PCR product (nt 51 to 6298) spanning the far left end of the viral genome. Based on the sequence (40), a 6.2-kb DNA fragment would be detected with the probe. Radioactivity was detected and quantitated with a STORM imaging system.

lytically infected BHK-21 cells (Fig. 3A, lane 2). Expression of most proteins peaked at 24 h posttransfection, although some proteins were visible as early as 12 h posttransfection. No viral lytic proteins were detected in pcDNA3-transfected S11E cells at any time posttransfection (Fig. 3B). Because 10^5 S11E cells with a 10% transfection efficiency were loaded in each lane (Fig. 3A, lanes 4 to 6), we found that much stronger signals were detected in a similar number of infected BHK-21 cells (10^4) in the control (Fig. 3A, lane 2), indicating higher levels of lytic protein expression in these cells. It was also noted that one lytic protein (Fig. 3A, indicated with an asterisk) was expressed at high levels in infected BHK-21 cells, but was not detected in S11E cells transfected with pcDNA3/MHV-68 *rta*.

Northern analyses were also performed to examine lytic gene transcription in transfected S11E cells. The kinetics of TK and M9 gene expression after Rta transfection are shown in Fig. 4. As described earlier, five major TK-related transcripts were seen in lytically infected BHK-21 cells (Fig. 2B), and a similar pattern of TK transcripts was also detected in S11E cells transfected with pcDNA3/MHV-68 *rta* (Fig. 4A, lanes 6 to 9), but not in cells transfected with pcDNA3 (Fig. 4A, lanes 2 to 5). The 2.6- and 3.2-kb transcripts expressed as early transcripts in lytically infected BHK-21 cells (Fig. 2B) were induced to a high level as early as 12 h posttransfection, and their expression decreased at 24 h posttransfection. The other TK-related RNAs, expressed as late viral transcripts in lytically infected BHK-21 cells (Fig. 2B), were visible at 12 h posttransfection, but continued to accumulate until 24 h posttransfection.

The same membrane was stripped and rehybridized with the M9 ORF probe (Fig. 4B). In lytically infected BHK-21 cells, the major 0.9- and 3.6-kb M9 transcripts were expressed as late viral RNAs (Fig. 2C). As seen in Fig. 4B, transfection of pcDNA3/MHV-68 *rta* (Fig. 4B, lanes 6 to 9), but not of pcDNA3 (Fig. 4B, lanes 2 to 5), led to expression of 0.9- and 3.6-kb M9 transcripts in S11E cells. The transcripts accumulated to high levels at 24 h posttransfection. Two minor M9 RNAs seen in lytically infected BHK-21 cells were, however, only detected at very low levels in S11E cells transfected with pcDNA3/MHV-68 *rta*.

MHV-68 Rta induced viral DNA replication in latently infected S11E cells. Since transfection of pcDNA3/MHV-68 *rta* activated some late viral transcripts, such as those of M9, the expression of which was demonstrated earlier to be dependent on viral DNA replication in lytically infected BHK-21 cells (Fig. 2C, lanes 10 and 11), viral DNA replication might also have been induced in S11E cells transfected with pcDNA3/MHV-68 *rta*. To confirm this, viral DNA replication was analyzed by Southern blotting. As seen in Fig. 5, viral DNA in S11E cells was greatly amplified by transfection of pcDNA3/MHV-68 *rta* (lanes 6 to 8), but not by pcDNA3 (lanes 3 to 5). At 24 h posttransfection, a 90-fold increase in the amount of viral DNA in pcDNA3/MHV-68 *rta*-transfected cells was detected compared to the amount in untransfected cells (Fig. 5, lanes 2 and 6). Given that the transfection efficiency was 10%, this would be an average of 900-fold induction of viral DNA synthesis in each transfected cell.

To confirm that the increase in viral DNA by Rta transfection was due to the induction of viral lytic DNA replication rather than amplification of the viral latent genome, a terminal repeat assay (31) was performed. The linear MHV-68 genome has multiple 1.2-kb tandem repeats at each terminus. In latently infected S11E cells, the MHV-68 genome exists as an episomal circular DNA generated by fusion through the ter-

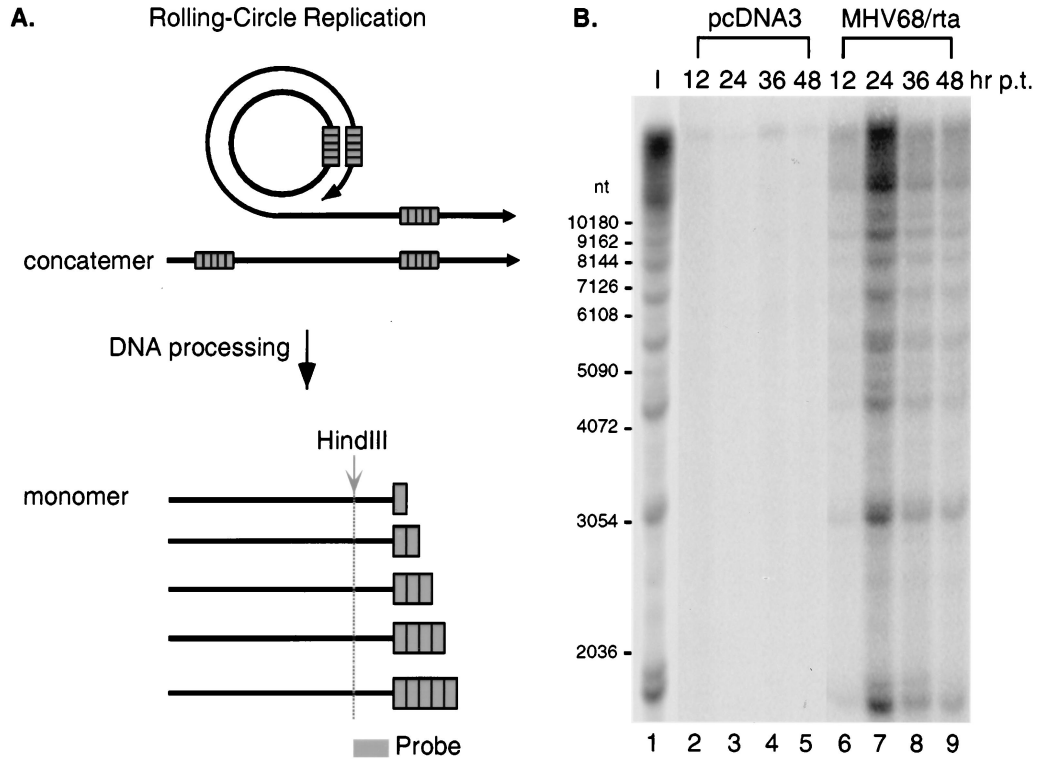

FIG. 6. Induction of lytic replication and processing of viral DNA by Rta. (A) The basis of the terminal repeat assay. The solid lines represent the double-stranded viral genome, and the boxes represent terminal repeats. In panel A, a rolling-circle mechanism is illustrated at the top, and the right ends of monomeric viral genomes after DNA processing are shown at the bottom. Since DNA processing can occur at any one of the terminal repeats between monomeric viral genomes on concatemers, there will be various numbers of repeats, with as few as one, at the termini of monomeric viral genomes. The gray arrow and dotted line indicate where digestions of *Hin*dIII occur adjacent to the terminal repeats. The shaded box indicates the position of the probe used for panel B. The details are further described in the text. (B) The results of the terminal repeat assay. Total DNA from 10^6 S11E cells transfected with pcDNA3 (lanes 2 to 5) or pcDNA3/MHV-68 *rta* (lanes 6 to 9) was harvested at 12 (lanes 2 and 6), 24 (lanes 3 and 7), 36 (lanes 4 and 8), or 48 (lanes 5 and 9) h posttransfection (p.t.). DNA was digested with *Hin*dIII and subjected to Southern analysis with a probe (its relative position is indicated in panel A) derived from a 0.8-kb PCR product (nt 118314 to 117560). Lane 1 is the positive control from the DNA of 10^5 MHV-68-infected BHK-21 cells digested with *Hin*dIII (I). Indicated to the left are the sizes of individual bands in a 1-kb DNA ladder. Radioactivity was detected with a STORM imaging system.

mini of the linear form (38). As illustrated in Fig. 6A, the terminal repeat assay is based on the fact that herpesviral DNA is replicated via a rolling-circle mechanism during the lytic cycle. Monomers of viral genomic DNA with variable numbers of terminal repeats are produced as a result of DNA cleavage at any one of the terminal repeats between monomeric viral genomes on concatemers. After digestion of viral DNA with *Hin*dIII (not present in the repeat) and probing with a unique region adjacent to terminal repeats, a 1.2-kb ladder of DNA fragments would be generated, due to variable numbers of repeats at the terminus. If lytic replication does not occur, after digestion of circular viral DNA, a single large DNA fragment containing the fused termini that harbors multiple copies of terminal repeats would be detected on Southern blots. The results of the terminal repeat assay are shown in Fig. 6B. Since viral DNA was greatly increased by Rta at 24 h posttransfection (Fig. 5), DNA was harvested at an additional time point at 12 h posttransfection. In S11E cells transfected with pcDNA3, only a large DNA fragment (≥23 kb) was detected at all time points (Fig. 6B, lanes 2 to 5), indicating that lytic replication did not occur. However, the DNA of cells transfected with pcDNA3/MHV-68 *rta* gave rise to ladders similar to those seen in lytically infected BHK-21 cells (Fig. 6B, lane 1). The intensity of DNA laddering was increased between 12 and 24 h posttransfection and then declined. These results provide evidence that transfection of Rta induced lytic replication of viral DNA and processing of the replicated viral DNA.

MHV-68 Rta transfection led to production of infectious viral particles from latently infected S11E cells. We have shown that introduction of MHV-68 Rta into S11E cells activated viral lytic gene expression and DNA replication. We further tested whether Rta was sufficient to drive the viral lytic cycle to production of viruses. The supernatants from transfected S11E cells were collected at various time points, and the viral titers were measured by plaque assays. The results are shown in Fig. 7. The viral titers in the supernatants from Rta-transfected S11E cells were much higher than in those from pcDNA3-transfected S11E cells. At 48 h posttransfection, there were ~130-fold more infectious viruses in the supernatant from Rta-transfected S11E cells.

DISCUSSION

Previous studies have shown the central roles of HHV-8 or EBV Rta in the switch from viral latency to lytic replication. Since the *rta* gene is highly conserved among gammaherpesviruses, we studied the gene expression and functions of MHV-68 *rta* in cell cultures. MHV-68 *rta* was expressed as an immediate-early gene during de novo lytic infection of BHK-21

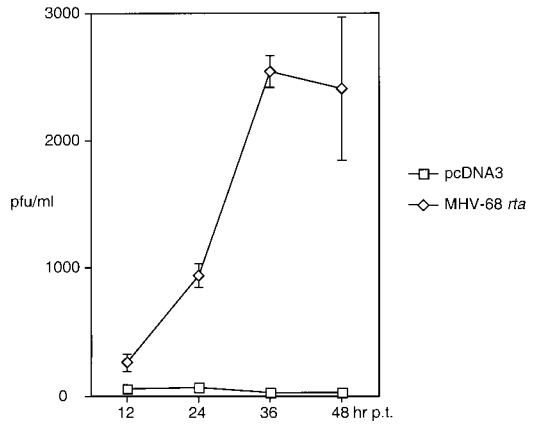

FIG. 7. Production and release of infectious viruses induced by Rta. At the times indicated at the bottom of the diagram, 10 ml of suspension cultures of S11E cells transfected with pcDNA3 (squares) or pcDNA/MHV-68 *rta* (diamonds) was centrifuged twice to remove cells, and the supernatants were collected for plaque assays to measure the viral titers. The data, including standard deviations indicated with error bars, were obtained from two or three independent assays and are expressed as PFU per milliliter of supernatant.

cells. Furthermore, exogenous expression of Rta activated the virus from latency in S11E cells harboring latent MHV-68. Our results have provided a foundation for studying the molecular mechanisms controlling establishment, maintenance, and disruption of latency in vivo.

Our analysis of the MHV-68 *rta* gene demonstrates that an 866-nt intron containing the entire ORF49 is spliced, generating the Rta ORF of 583 aa with the initiation methionine at nt 66760 (Fig. 1). 5′ rapid amplification of cDNA ends was also carried out on the polyadenylated RNA, and the preliminary data localized the 5′ end of the *rta* transcript at ~100 nt upstream of the initiation methionine of the Rta ORF (data not shown). Taken together with a consensus poly(A) signal located 57 nt after the termination codon, the size of the spliced *rta* RNA is estimated to be ~1.9 kb, consistent with the size of the major immediate-early *rta* transcript (2 kb) detected in lytically infected BHK-21 cells (Fig. 2A). However, the nature of the other minor transcripts requires further investigation.

The *rta* genes of gammaherpesviruses share similarities in the genomic location, amino acid sequence, and splicing pattern, which suggests that Rta plays a conserved and important role in the life cycle of the virus. However, among gammaherpesviruses, there are differences in terms of the location of the initiation methionine and the nature of the *rta* transcript. Except for EBV (19), the initiation methionines of Rta in MHV-68, HHV-8 (17, 35), HVS (42), and BHV-4 (39) are located in the first rather than the second exon. Thus, EBV Rta is entirely encoded by ORF50 (19), whereas the Rta proteins of the other gammaherpesviruses have extra amino acids added to the N terminus of ORF50. The *rta* transcripts of MHV-68, HVS, and BHV-4 are monocistronic (39, 41), whereas the EBV *rta* transcript is bicistronic, with an additional ORF encoding ZEBRA downstream of the *rta* ORF (19). The HHV-8 *rta* transcript is polycistronic, with not only the K8 ORF encoding the ZEBRA homologue (10, 16, 17, 35, 46), but also the putative K8.2 ORF downstream of the K8 ORF (46). It is not clear whether ZEBRA of EBV or HHV-8 can be translated from either the bicistronic or polycistronic message. No ZEBRA homologue has been identified in MHV-68, HVS, or BHV-4.

MHV-68 Rta most likely functions as a transcriptional activator. Homologues of Rta from other gammaherpesviruses such as EBV, HVS, and BHV-4 have been shown to activate the promoters of viral early genes in transient transfection assays (1, 9, 11, 12, 24, 39). Amino acid sequence alignments of the Rta homologues reveal that the most conserved region is at the N terminus. This conserved portion of EBV Rta is required for dimerization and DNA binding (20). Another well-conserved region is at the C terminus and is rich in acidic residues, which is characteristic of activation domains of many transcriptional activators. It has been shown that this region of EBV Rta is essential for transcriptional activation (20). Therefore, the Rta homologues of gammaherpesviruses share similar amino acid sequences and may also have similar functions in activating viral and possibly cellular promoters. However, it is not clear whether the Rta proteins are capable of substituting for each other to transactivate virus-specific promoters. It has been shown that BHV-4 Rta could not transactivate the viral promoters that were activated by either HVS or EBV Rta, nor could EBV Rta transactivate the viral promoters that were activated by either BHV-4 or HVS Rta (39). This specificity suggests that despite the conservation of the functions in transactivation, virus- or host-specific interactions may be involved in mediating such functions.

MHV-68 Rta alone was sufficient to reactivate the virus in B cells. Transfection of an Rta expression plasmid induced the expression of early and late viral RNAs and proteins, activated lytic replication of viral DNA, and led to the production and release of infectious viral particles. So far, no other reports have demonstrated that Rta alone is sufficient to drive the progression of the viral lytic cycle to the production of infectious virions. In our time course experiments (Fig. 4), the lytic gene expression induced by Rta in S11E cells proceeded in a cascade similar to that observed in de novo lytic infection of BHK-21 cells (Fig. 2). After Rta transfection, the early 2.6-kb TK transcript was expressed to a high level at 12 h posttransfection, followed by the late 0.9- and 3.6-kb M9 transcripts, peaking at 24 h posttransfection (Fig. 4). The highest level of viral DNA was observed at 24 h posttransfection (Fig. 5 and 6), followed by the maximal accumulation of infectious particles in the supernatants occurring at 36 h posttransfection (Fig. 7). Nevertheless, we noticed that there was significantly more intensive viral lytic replication in de novo-infected BHK-21 cells than in S11E cells transfected by pcDNA3/MHV-68 *rta*. Differences in the replication levels between the two cell types may be due to a suboptimal microenvironment in B cells for viral lytic replication. This interpretation is consistent with the predominantly latent nature of B-cell infection. We also observed that one major lytic viral protein expressed in de novo-infected BHK-21 cells was not seen in S11E cells transfected by pcDNA3/MHV-68 *rta*. Because the antibody used for Western analysis is polyclonal, the identity of this viral protein is not clear. However, since there are infectious particles produced and released into the medium, the viral protein not detected in Rta-induced reactivation is unlikely to be essential for viral replication in B cells.

Based on our results that *rta* was expressed as an immediate-early gene during de novo lytic infection and that transfection of an Rta expression plasmid induced the viral lytic cycle in latently infected B cells, we propose a working model for the functions of MHV-68 Rta. In this model, Rta is the central viral factor determining lytic replication or latency of MHV-68. During de novo infection of permissive cells such as BHK-21, Rta, presumably activated by cooperation between a virion protein similar to HSV VP16 and cellular transcription factors, is expressed to drive the viral lytic cycle. In nonpermissive cells

such as B cells, Rta expression is blocked, which prevents initiation of the viral lytic cascade, leading to latency. Sustained latency may require expression of viral latent genes. However, in response to certain stimuli, Rta expression is either activated or derepressed, and then latency is disrupted and the virus undergoes reactivation. This model strongly points to regulation of Rta expression governing the balance between viral latency and lytic replication. Moreover, controlling the expression of Rta may allow us to tip the balance between latency and lytic replication. Therefore, MHV-68 offers a unique model system in which to study the consequences of such a balance to viral pathogenesis.

ACKNOWLEDGMENTS

We thank Helen Brown, Tammy Rickabaugh, and Tonia Symensma for critical comments and Wendy Aft for editing the manuscript.

This work is supported by the Frontiers of Science Award. T.-T.W. is supported by a fellowship from Cancer Research Institute. E.J.U. is supported by NIH grant AI37597. J.P.S. is a Royal Society University Research Fellow.

REFERENCES

1. **Buisson, M., E. Manet, M.-C. Trescol-Biemont, H. Gruffat, B. Durand, and A. Sergeant.** 1989. The Epstein-Barr virus (EBV) early protein EB2 is a posttranscriptional activator expressed under the control of EBV transcription factors EB1 and R. J. Virol. **63:**5276–5284.
2. **Chevallier-Greco, A., H. Gruffat, E. Manet, A. Calender, and A. Sergeant.** 1989. The Epstein-Barr virus (EBV) DR enhancer contains two functionally different domains: domain A is constitutive and cell specific, domain B is transactivated by the EBV early protein R. J. Virol. **63:**615–623.
3. **Chevallier-Greco, A., E. Manet, P. Chavrier, C. Mosnier, J. Daillie, and A. Sergeant.** 1986. Both Epstein-Barr virus (EBV)-encoded trans-acting factors, EB1 and EB2, are required to activate transcription from an EBV early promoter. EMBO J. **5:**3243–3249.
4. **Chomczynski, J. M., and N. Sacchi.** 1987. Single-step method of RNA isolation by acid guanidinium thiocyanate-phenol-chlorofom extraction. Anal. Biochem. **162:**156.
5. **Countryman, J., and G. Miller.** 1985. Activation of expression of latent Epstein-Barr herpesvirus after gene transfer with a small cloned subfragment of heterogeneous viral DNA. Proc. Natl. Acad. Sci. USA **82:**4085–4089.
6. **Cox, M. A., J. Leahy, and J. M. Hardwick.** 1990. An enhancer within the divergent promoter of Epstein-Barr virus responds synergistically to the R and Z transactivators. J. Virol. **64:**313–321.
7. **Farrell, R. E. J.** 1993. RNA methodologies. Academic Press, Inc., San Diego, Calif.
8. **Flemington, E., and S. H. Speck.** 1990. Autoregulation of Epstein-Barr virus putative lytic switch gene BZLF1. J. Virol. **64:**1227–1232.
9. **Gruffat, H., E. Manet, A. Rigolet, and A. Sergeant.** 1990. The enhancer factor R of Epstein-Barr virus (EBV) is a sequence-specific DNA binding protein. Nucleic Acids Res. **18:**6835–6843.
10. **Gruffat, H., S. Portes-Sentis, A. Sergeant, and E. Manet.** 1999. Kaposi's sarcoma-associated herpesvirus (human herpesvirus-8) encodes a homologue of the Epstein-Barr virus bZip protein EB1. J. Gen. Virol. **80:**557–561.
11. **Hardwick, J. M., P. M. Lieberman, and S. D. Hayward.** 1988. A new Epstein-Barr virus transactivator, R, induces expression of a cytoplasmic early antigen. J. Virol. **62:**2274–2284.
12. **Holley-Guthrie, E. A., E. B. Quinlivan, E.-C. Mar, and S. Kenney.** 1990. The Epstein-Barr virus (EBV) BMRF1 promoter for early antigen (EA-D) is regulated by the EBV transactivators, BRLF1 and BZLF1, in a cell-specific manner. J. Virol. **64:**3753–3759.
13. **Husain, S. M., E. J. Usherwood, H. Dyson, C. Coleclough, M. A. Coppola, D. L. Woodland, M. A. Blackman, J. P. Stewart, and J. T. Sample.** 1999. Murine gammaherpesvirus M2 gene is latency-associated and its protein a target for CD8(+) T lymphocytes. Proc. Natl. Acad. Sci. USA **96:**7508–7513.
14. **Kenney, S., E. Holley-Guthrie, E.-C. Mar, and M. Smith.** 1989. The Epstein-Barr virus BMLF1 promoter contains an enhancer element that is responsive to the BZLF1 and BRLF1 transactivators. J. Virol. **63:**3878–3883.
15. **Lieberman, P. M., J. M. Hardwick, J. Sample, G. S. Hayward, and S. D. Hayward.** 1990. The Zta transactivator involved in induction of lytic cycle gene expression in Epstein-Barr virus-infected lymphocytes binds to both AP-1 and ZRE sites in target promoter and enhancer regions. J. Virol. **64:**1143–1155.
16. **Lin, S.-F., D. R. Robinson, G. Miller, and H.-J. Kung.** 1999. Kaposi's sarcoma-associated herpesvirus encodes a bZIP protein with homology to BZLF1 of Epstein-Barr virus. J. Virol. **73:**1909–1917.
17. **Lukac, D. M., R. Renne, J. R. Kirshner, and D. Ganem.** 1998. Reactivation of Kaposi's sarcoma-associated herpesvirus infection from latency by expression of the ORF 50 transactivator, a homolog of the EBV R protein. Virology **252:**304–312.
18. **Mackett, M., J. P. Stewart, S. D. Pepper, M. Chee, S. Efstathiou, A. A. Nash, and J. R. Arrand.** 1997. Genetic content and preliminary transcriptional analysis of a representative region of murine gammaherpesvirus 68. J. Gen. Virol. **78:**1425–1433.
19. **Manet, E., H. Gruffat, B. M. C. Trescol, N. Moreno, P. Chambard, J. F. Giot, and A. Sergeant.** 1989. Epstein-Barr virus bicistronic mRNAs generated by facultative splicing code for two transcriptional trans-activators. EMBO J. **8:**1819–1826.
20. **Manet, E., A. Rigolet, H. Gruffat, J. F. Giot, and A. Sergeant.** 1991. Domains of the Epstein-Barr virus (EBV) transcription factor R required for dimerization, DNA binding and activation. Nucleic Acids Res. **19:**2661–2667.
21. **Mellinghoff, I., M. Daibata, R. E. Humphreys, C. Mulder, K. Takada, and T. Sairenji.** 1991. Early events in Epstein-Barr virus genome expression after activation: regulation by second messengers of B cell activation. Virology **185:**922–928.
22. **Nash, A. A., and N. P. Sunil-Chandra.** 1994. Interactions of the murine gammaherpesvirus with the immune system. Curr. Opin. Immunol. **6:**560–563.
23. **Nash, A. A., E. J. Usherwood, and J. P. Stewart.** 1996. Immunological features of murine gammaherpesvirus infection. Semin. Virol. **7:**125–130.
24. **Nicholas, J., L. S. Coles, C. Newman, and R. W. Honess.** 1991. Regulation of the herpesvirus saimiri (HVS) delayed-early 110-kilodalton promoter by HVS immediate-early gene products and a homolog of the Epstein-Barr virus R *trans* activator. J. Virol. **65:**2457–2466.
25. **Packham, G., M. Brimmell, D. Cook, A. J. Sinclair, and P. J. Farrell.** 1993. Strain variation in Epstein-Barr virus immediate early genes. Virology **192:**541–550.
26. **Pepper, S. D., J. P. Stewart, J. R. Arrand, and M. Mackett.** 1996. Murine gammaherpesvirus-68 encodes homologues of thymidine kinase and glycoprotein H: sequence, expression, and characterization of pyrimidine kinase activity. Virology **219:**475–479.
27. **Quinlivan, E. B., E. A. Holley-Guthrie, M. Norris, D. Gutsch, S. L. Bachenheimer, and S. C. Kenney.** 1993. Direct BRLF1 binding is required for cooperative BZLF1/BRLF1 activation of the Epstein-Barr virus early promoter, BMRF1. Nucleic Acids Res. **21:**1999–2007.
28. **Ragoczy, T., L. Heston, and G. Miller.** 1998. The Epstein-Barr virus Rta protein activates lytic cycle genes and can disrupt latency in B lymphocytes. J. Virol. **72:**7978–7984.
29. **Rickinson, A. B., and E. Kieff.** 1996. Epstein-Barr virus, 3rd ed., vol. 2. Lippincott-Raven Publishers, Philadelphia, Pa.
30. **Sarawar, S. R., R. D. Cardin, J. W. Brooks, M. Mehrpooya, R. A. Tripp, and P. C. Doherty.** 1996. Cytokine production in the immune response to murine gammaherpesvirus 68. J. Virol. **70:**3264–3268.
31. **Sato, H., T. Takimoto, S. Tanaka, J. Tanaka, and N. Raab-Traub.** 1990. Concatameric replication of Epstein-Barr virus: structure of the termini in virus-producer and newly transformed cell lines. J. Virol. **64:**5295–5300.
32. **Sinclair, A. J., M. Brimmell, F. Shanahan, and P. J. Farrell.** 1991. Pathways of activation of the Epstein-Barr virus productive cycle. J. Virol. **65:**2237–2244.
33. **Stevenson, P. G., and P. C. Doherty.** 1998. Kinetic analysis of the specific host response to a murine gammaherpesvirus. J. Virol. **72:**943–949.
34. **Stewart, J. P., N. J. Janjua, S. D. V. Pepper, G. Bennion, M. Mackett, T. Allen, A. A. Nash, and J. R. Arrand.** 1999. Identification and characterization of murine gammaherpesvirus 68 gp150: a virion membrane glycoprotein. J. Virol. **70:**3528–3535.
35. **Sun, R., S. F. Lin, L. Gradoville, Y. Yuan, F. Zhu, and G. Miller.** 1998. A viral gene that activates lytic cycle expression of Kaposi's sarcoma-associated herpesvirus. Proc. Natl. Acad. Sci. USA **95:**10866–10871.
36. **Sunil-Chandra, N. P., S. Efstathiou, J. Arno, and A. A. Nash.** 1992. Virological and pathological features of mice infected with murine gamma-herpesvirus 68. J. Gen. Virol. **73:**2347–2356.
37. **Takada, K., and Y. Ono.** 1989. Synchronous and sequential activation of latently infected Epstein-Barr virus genomes. J. Virol. **63:**445–449.
38. **Usherwood, E. J., J. P. Stewart, and A. A. Nash.** 1996. Characterization of tumor cell lines derived from murine gammaherpesvirus-68-infected mice. J. Virol. **70:**6516–6518.
39. **van Santen, V. L.** 1993. Characterization of a bovine herpesvirus 4 immediate-early RNA encoding a homolog of the Epstein-Barr virus R transactivator. J. Virol. **67:**773–784.
40. **Virgin, H. W., IV, P. Latreille, P. Wamsley, K. Hallsworth, K. E. Weck, A. J. Dal Canto, and S. H. Speck.** 1997. Complete sequence and genomic analysis of murine gammaherpesvirus 68. J. Virol. **71:**5894–5904.
41. **Whitehouse, A., I. M. Carr, J. C. Griffiths, and D. M. Meredith.** 1997. The herpesvirus saimiri ORF50 gene, encoding a transcriptional activator homologous to the Epstein-Barr virus R protein, is transcribed from two distinct promoters of different temporal phases. J. Virol. **71:**2550–2554.
42. **Whitehouse, A., A. J. Stevenson, M. Cooper, and D. M. Meredith.** 1997. Identification of a cis-acting element within the herpesvirus saimiri ORF 6

promoter that is responsive to the HVS.R transactivator. J. Gen. Virol. **78:**1411–1415.
43. **Whitley, R. J.** 1996. Herpes simplex virus, p. 2297–2342. *In* B. N. Fields, D. M. Knipe, and P. M. Howley (ed.), Fields virology, 3rd ed, vol. 2. Lippincott-Raven Publishers, Philadelphia, Pa.
44. **Zalani, S., E. Holley-Guthrie, and S. Kenney.** 1996. Epstein-Barr viral latency is disrupted by the immediate-early BRLF1 protein through a cell-specific mechanism. Proc. Natl. Acad. Sci. USA **93:**9194–9199.
45. **Zalani, S., E. A. Holley-Guthrie, D. E. Gutsch, and S. C. Kenney.** 1992. The Epstein-Barr virus immediate-early promoter BRLF1 can be activated by the cellular Sp1 transcription factor. J. Virol. **66:**7282–7289.
46. **Zhu, F. X., T. Cusano, and Y. Yuan.** 1999. Identification of the immediate-early transcripts of Kaposi's sarcoma-associated herpesvirus. J. Virol. **73:** 5556–5567.